J. Environ. Nanotechnol.
Volume 3, No.4 (2014) pp. 105-111
ISSN (Print): 2279-0748
ISSN (Online): 2319-5541
doi: 10.13074/jent.2014.12.144132

Enhanced Methylene Blue Dye Degradation by Newly Synthesized Ag_2O/TiO_2 Heterostructure

D. Sriprabha[1], T. Mohankumar[2], D. Nataraj[3], T. Daniel Thangadurai[4]*

[1,2,4*]Department of Nanotechnology, Sri Ramakrishna Engineering College, Coimbatore, TN, India.
[3]Department of Physics, Bharathiar University, Coimbatore, TN, India.

Received:03.09.2014 Accepted:15.12.2014

Abstract

Silver (Ag) coated TiO_2 heterostructure was prepared by precipitation method using equal ratio of silver nitrate ($AgNO_3$) and as-synthesized TiO_2 nanobelt. The X-ray diffraction study results indicate high crystalline nature of the Ag_2O/TiO_2 heterostructure. The surface morphology of Ag_2O/TiO_2 heterostructure has thoroughly been investigated by Scanning Electron Microscopy (SEM). The stability and thermal studies of Ag_2O/TiO_2 heterostructure were examined by using Zeta analyzer and Differential Scanning Calorimetry, respectively. Photocatalytic activity studies were carried out using Methylene Blue (MB) as a model molecule to highlight the consequence of Ag_2O/TiO_2 heterostructure. The reuse of Ag_2O/TiO_2 nanobelt after annealing shows the excellent recovery of the catalyst. These studies may contribute to additional applications of hierarchical Ag_2O/TiO_2 heterostructure membranes, including harnessing sunlight for water treatment and photo catalytic activity.

Keywords: *Ag2O/TiO2 heterostructure; Hydrothermal process; Methylene blue; Precipitation method; Photo catalytic activity.*

1. INTRODUCTION

TiO_2 is regarded as the most efficient and environmentally benign photocatalyst. During the last three decades, titanium dioxide (TiO_2) has been comprehensively studied as a wide-band-gap photocatalyst (Xiong and Zhao, 2012; Wang *et al*. 2009; Liu *et al*. 2012; Hegde *et al*. 2005) Wide-band gap semiconductor TiO_2 nanobelt has potential use as components in electronic and optical devices because of their transparency and high carrier excitation energy. The goal of research in this area is to look for efficient materials for photocatalytic processes, including the photocatalytic decomposition of various pollutants, and killing bacteria. There is a range of recent studies suggesting other possible applications of Ti–O nano materials (Zhou *et al.* 2010).

Loading of noble metal particles, such as platinum, gold, and palladium on TiO_2 photocatalysts can improve photocatalytic activities (Henderson *et al*. 2003). Especially, the deposition of silver (Ag) nanoparticles on TiO_2 photocatalyst can highly improve its photocatalytic efficiency through the Schottky barrier conduction band electron trapping and consequent longer electron-hole pair lifetimes; (Linsebigler *et al*. 1995). Ag coated TiO_2 catalysts have many industrial applications such as epoxidation, oxi-dehydrogenation, as well as the low-temperature selective oxidation (Zhou *et al*. 2004) At the same time, the Ag_2O/TiO_2 heterostructure also has a towering visible photocatalytic activity. The enhancement is attributed to the fact that the loading of Ag results in the formation of Schotty barriers at each Ag–TiO2 contact regions, thus promoting charge separation and inhibiting the recombination of electron–hole pairs, leaving holes in the valence band of TiO_2 (Zhou *et al*. 2004). Ag_2O/TiO_2 heterostructure can effectively suppress the rate of electron-hole recombination under ultra violet (UV) light irradiation.

The principle of the semiconductor photocatalytic reaction is straightforward. Upon absorption of photons with energy larger than the band gap of TiO_2, electrons are excited from the valence band to the conduction band, creating electron–hole pairs. These charge carriers migrate to

* **T. Daniel Thangadurai** **Tel.no:** +91-422-246-1588
E-mail: danielt@srec.ac.in

the surface and react with the chemicals adsorbed on the surface to decompose them. The holes or the surface hydroxyl radicals are generally viewed as major oxidizing agents for degrading reactants, while superoxide anions formed by scavenging the electrons from the conduction band are also capable of oxidizing reactants (Dodda *et al*. 2007). In this paper, we demonstrate that Ag_2O/TiO_2 heterostructure can be used as an efficient electron absorbing agent under UV light irradiation and as an efficient photosensitizer under visible light irradiation in photocatalysis system. Ag nanoparticles were loaded on the surface of TiO_2 nanobelts by co-precipitation method to form Ag_2O/TiO_2 heterostructure. TiO_2 nanobelts were chosen as the test material, because one-dimensional nanostructures have advantages over nano particles, such as enhanced visible-light scattering and absorption, rapid diffusion-free electron transport along the long direction; and the low number of grain boundaries.

2. EXPERIMENTAL METHODS

2.1 Materials & Methods

All chemicals and solvents were of analytical grade and purchased from commercial sources. TiO_2, NaOH, HCl, $AgNO_3$ are purchased from Sigma Aldrich and Merck, used without any further purification.

Infra red spectra of nanobelt samples were recorded on Bruker ATR-FTIR spectrometer (Bruker Alpha – T, Germany). UV–Visible measurements were made on Analytik Jena spectrophotometer (Model SZ-100, Germany) at 298 K. Zeta potential was analyzed on Zeta analyzer (Horiba SZ-100Z, Japan) with PMT detector. The thermal stability of nanobelt was investigated by Differential Scanning Calorimetry (DSC Q20V 24) in an air stream at a heating rate of 10 °C/min. Fluorescence experiments were performed in Horiba Fluoromax-4 spectrofluorometer. The pH measurements were carried out using digital pH instrument (HANNA, Romania). X-ray diffraction studies were performed on Xpert Powder diffractometer (Pananlytical, The Netherlands) with Cu Kα (λ = 0.15406 nm). Scanning Electron Microscope (SEM) analysis was carried out using Qunata 250 model (FEI, Czech Republic) with Tungsten as electron source and Everhart Thornley Detector as detector.

2.2 Preparation of TiO_2 nanobelt

Titanate nanobelt was synthesized by the hydrothermal process in concentrated NaOH aqueous solution. A commercial anatase TiO_2 powder was used as the precursor, and a typical procedure is as follows: TiO_2 powder (0.1 g) was mixed with 20 mL of 10 M NaOH aqueous solution, followed by hydrothermal treatment at 200 ^oC in a Teflon-lined autoclave for 48 h (eq. 1). The resulted powder was washed thoroughly with deionized water followed by filtration and rying process. The obtained sodium titanate nanobelts (Wang *et al.* 2008) were dipped in 0.1 M HCl aqueous solution for 24 h and then washed thoroughly with water to get hydrogen titanate nanobelts (eq. 2). By annealing the hydrogen titanate at 500 ^oC for 1 h, anatase TiO_2 nanobelts were obtained (eq. 3).

$$3TiO_2 + 2NaOH \rightarrow Na_2Ti_3O_7 + H_2O \quad (1)$$

$$Na_2Ti_3O_7 + 2HCl \rightarrow H_2Ti_3O_7 + 2NaCl \quad (2)$$

$$H_2Ti_3O_7 \rightarrow 3TiO_2 + H_2O \quad (3)$$

$Na_2Ti_3O_7$ and $H_2Ti_3O_7$ are closely related structures. $Na_2Ti_3O_7$ is a layered structure composed of $[TiO_6]$ octahedra with shared edges and vertices. The Na+ cations are located between the $[TiO_6]$ layers. If $Na_2Ti_3O_7$ is soaked and washed with a diluted acid solution, Na+ ions can be replaced by H_3O+ ions to form $H_2Ti_3O_7$. Therefore, $H_2Ti_3O_7$ nanobelts can be obtained from $Na_2Ti_3O_7$ nanobelts by ion exchange and anatase TiO_2 can be obtained by heat-treatment of $H_2Ti_3O_7$ at 500 ^oC for 1 h through dehydration and crystal-lattice rearrangement process.

2.3 Preparation of Ag_2O/TiO_2 heterostructure

Ag_2O/TiO_2 heterostructure was prepared by the precipitation method. 0.12 g of newly synthesized TiO_2 nanobelts were dispersed in 50 mL of distilled water and 0.27 g of $AgNO_3$ was added to the suspension. The mixture was stirred magnetically for 30 min. 50 mL of 8.0 M NaOH was added drop wise to the above reaction mixture. The amount of NaOH was more than sufficient to precipitate Ag_2O from the added $AgNO_3$ (pH = 14). TiO_2 nanobelts coated by Ag_2O nanoparticles were centrifuged and washed thoroughly with deionized water followed by a filtration and drying.

2.4 Photocatalytic degradation of MB under UV and Visible- Light Irradiation

Methylene blue was chosen as the model organic compound to evaluate the photoactivity of the prepared Ag_2O/TiO_2 nanomaterials. In a typical experiment, 20 mL aqueous suspensions of MB (0.003 M) and 5 mg of Ag_2O/TiO_2 nanobelts powder were placed in a 50 mL beaker. Prior to irradiation, the suspension was vigorously stirred for 30 min to establish adsorption/desorption equilibrium (Hu *et al.* 2013). An 11 W UV lamp with a maximum emission at 254 nm was used as the UV resource for UV light photocatalysis and a 300 W Xe arc lamp was

used as the visible light source for visible-light photocatalysis. At given time intervals, 3 mL aliquots were sampled and centrifuged to remove the particles. The filtrates were analyzed by measuring the absorption band maximum (670 nm) using a UV-Vis spectrophotometer. The blank reaction was carried out following the same procedure without adding catalyst. Repeat tests were run to ensure data reliability.

3. RESULTS & DISCUSSION

The formation of $Na_2Ti_3O_7$ nanotubes at lower temperatures is due to large surface strain energy when surface hydrogen loss exceeds a critical value. However, in our experiment, the autoclaving temperature was much higher (180 ^oC), which leads to a higher growth rate of nanosheets, resulting in long nanobelts. It may require larger strain energy, but there is not enough strain energy for the surface layer to overcome the coupling with the underlying layer, which may be why no $Na_2Ti_3O_7$ nanotubes appear in our experiment.

3.1 X-ray diffraction studies

X-ray diffraction patterns of TiO_2 nanobelts and Ag_2O/TiO_2 heterostructure are shown in Fig. 1. All the diffraction peaks in the pattern of pure TiO_2 nanobelts can be indexed as anatase type structure (Fig. 1a). The diffraction peaks of the nanobelt sample are in good harmony with that reported in the literature, indicating the formation of the Ag-TiO_2 phase. The anatase TiO_2 diffraction pattern showed well resolved intense peaks (JCPDS 89-4203). After coupling with Ag, the crystal phase of TiO2 remained unchanged except a slight shift of 38.30° (200).

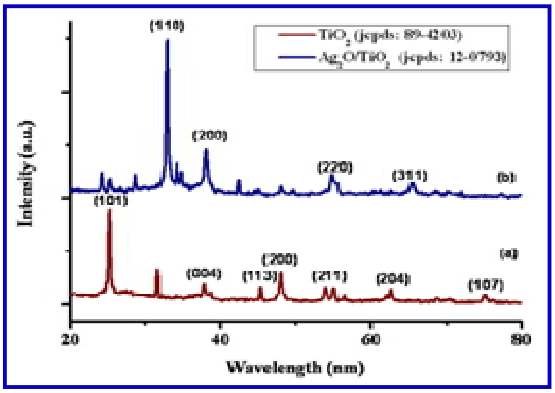

Fig. 1: (a) X-ray diffraction patterns of as-synthesized TiO2 nanobelt synthesized by sequential autoclaving at 200 ^oC in NaOH solution and (b) Ag2O/TiO2 nanobelt fabricated by precipitation method

The anatase TiO_2 and Ag_2O phases coexist in the Ag_2O/TiO_2 heterostructure crystals, and the XRD patterns match their JCPDS files (No. 12-0793). Furthermore, the appearance of new intense peak at 32.81° (110) confirms the formation of Ag_2O/TiO_2 heterostructure (Sze-Mun Lam *et al.* 2013). Other well-resolved sharp and intense peaks indicate Ag_2O/TiO_2 heterostructure have a relatively high degree of crystallinity.

3.2 Surface morphology studies

The morphology and microstructural features of as-synthesized TiO_2 nanobelt and Ag_2O/TiO_2 heterostructure were examined by using Scanning Electron Microscope (SEM). It can be seen that as-synthesized TiO_2 nanobelts consisted of ~115-190 nm in thickness and ~1.5-2.0μm in length (Fig. 2a). After coupling with Ag_2O, the thickness of the Ag_2O/TiO_2 heterostructure increased to ~210-225 nm width and ~2.0 μm length (Fig. 2b). The rough surfaces of TiO_2 nanobelts provide a very good phase to absorb Ag_2O nanoparticles in high capacity during the co-precipitation process. Considering the crystallographic symmetry of anatase nanorods, the dominant exposed facets can be identified as {101} planes, which are the most thermodynamically stable facets of anatase TiO_2 (Li *et al.* 2008; Mukhopadhyay *et al.* 2010) and constitute ~95% of the total exposed surface.

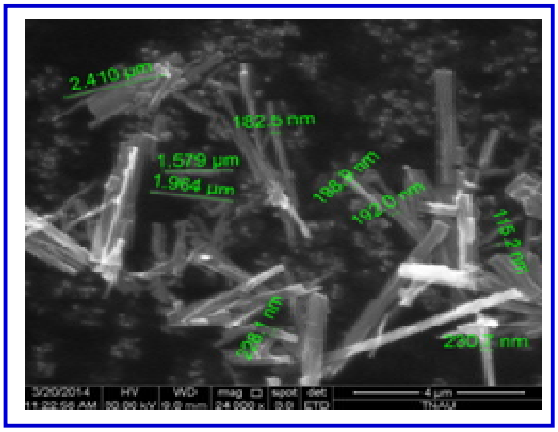

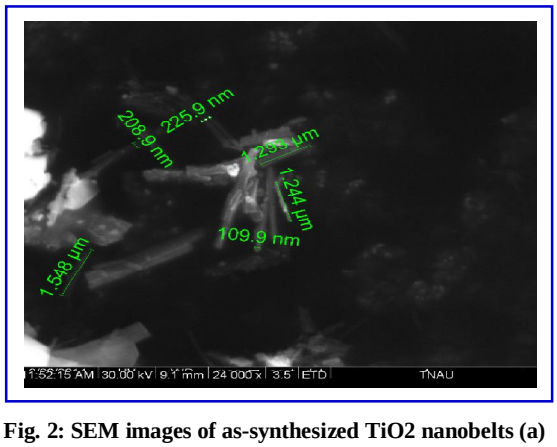

Fig. 2: SEM images of as-synthesized TiO2 nanobelts (a) and Ag2O/TiO2 heterostructure (b) with different magnification

3.3 Infra red and UV-Visible spectroscopy

The I.R. spectrum of newly synthesized Ag_2O/TiO_2 heterostructure was compared with that of TiO_2 nanobelt in order to elucidate the formation of Ag coated TiO_2 heterostructure. In the IR spectrum of Ag_2O/TiO_2 heterostructure, a strong band was observed at *ca.* 1640 and 1410 cm^{-1} which is characteristic of stretching and bending of O-Ti-O bond. The peaks at *ca.* 510 and 430 cm^{-1} for Ag-O and Ag/TiO_2 bonding, respectively (SI, Fig. S1), which confirms the formation of Ag_2O/TiO_2 heterostructure.

To corroborate the preparation of Ag_2O/TiO_2 heterostructure, UV-Visible absorption spectroscopy was carried out for as-synthesized TiO_2 nano belt, commericial TiO_2, $AgNO_3$ and Ag_2O/TiO_2 heterostructure at room temperature. The appearance of absorption band at *ca.* 380 nm for as-synthesized TiO_2 nanobelt confirms the preparation of TiO_2 nanobelt, which is in good agreement with commercially available sample (Fig. 3). The $AgNO_3$ sample showed the Ag characteristic band at *ca.* 410 nm; but in the Ag_2O/TiO_2 heterostructure absorption spectrum, the disappearance of both 380 and 410 nm absorption bands proves the formation of Ag_2O/TiO_2 heterostructure.

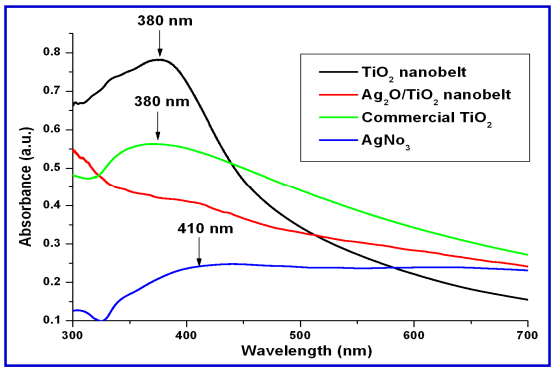

Fig. 3: UV-Visible absorption spectrum of as-synthesized TiO2, newly synthesized Ag2O/TiO2 heterostructure, commercial TiO2 and AgNO3 in water at 25 °C.

The Diffused Reflectance Spectra (DRS) of as-synthesized TiO_2 nanobelts and Ag_2O/TiO_2 heterostructure are shown in Figure 4. TiO_2 nanobelts exhibit a very steep absorption edge located at *ca.* 380 nm. In comparison to pure TiO_2 nanobelts, the absorption edge of Ag_2O/TiO_2 heterostructure red-shifts to about *ca.* 410 nm (Xu *et al.* 2012). The Ag_2O/TiO_2 heterostructure also exhibit a narrow absorption band around 450-700 nm which is assigned as Ti-O bond. The absorption above 450 nm in Ag_2O/TiO_2 heterostructure photocatalyst is attributed to the presence of Ag_2O nanoparticles as visible-light sensitization which has a strong and wide absorption band in the visible-light region.

3.4 Practical size analysis and Stability studies

The stability of Ag_2O/TiO_2 heterostructure was determined by calculating the zeta potential using zeta analyzer (Fig. 5) at room temperature. The zeta potential (0.1 mV) and electrophoretic mobility (0.000001 cm2/Vs) values indicates that the newly synthesized Ag_2O/TiO_2 nanobelt is highly stable, can be moveable with very less current and mono dispersed.

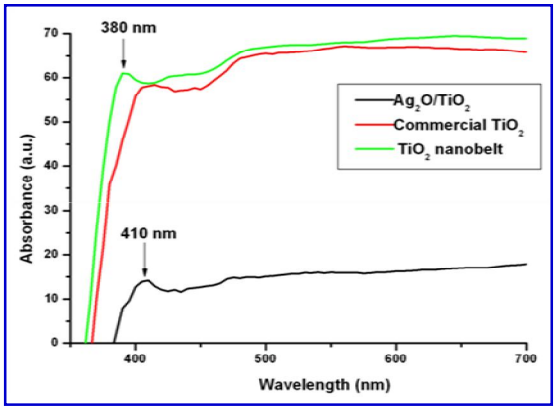

Fig. 4: Diffused reflectance spectrum of Ag_2O / TiO_2 heterostructure, commercial TiO_2 and as-synthesized TiO_2 nanobelts at 25 °C.

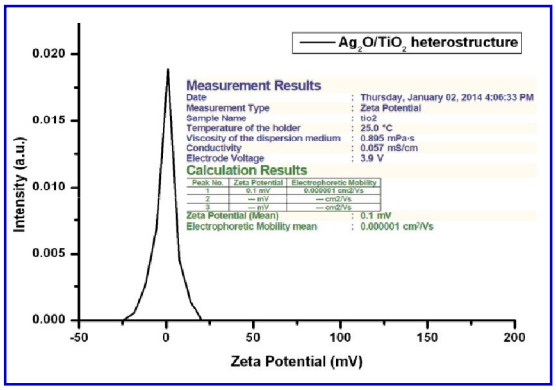

Fig. 5: Zeta potential analysis of synthesized Ag_2O / TiO_2 heterostructure in water at 25 °C.

3.5 Fluorescence studies

The separation and recombination of photoinduced charge carriers which is related to the transfer behavior of the photoinduced electrons and holes can be reflected in PL spectra. The PL spectra of TiO_2 nanobelts and Ag_2O/TiO_2 samples are shown in Fig. 6. The excitation wavelength is determined as 350 nm, and the pure TiO_2 nanobelts have a strong emission peak at *ca.* 405 nm. The PL intensities of Ag_2O/TiO_2 heterostructure decreased which is due to the Ag_2O nanoparticles deposited on the surface of

TiO_2 nanobelts act as traps to capture the photoinduced electrons, and thus inhibit recombination of electron-hole pairs (Lazzeri *et al*. 2001; Dai *et al*. 2009). The PL spectra result is in good agreement with the enhancement of photocatalytic activity of Ag_2O/TiO_2 nanobelts heterostructure under UV light.

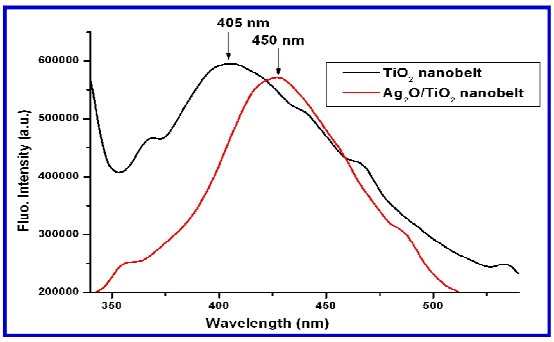

Fig.6: Fluorescence emission intensities of as-synthesized TiO_2 nanobelts and Ag_2O / TiO_2 heterostructure (excitation : 350 nm; slit width : 1 nm) in water at 25 °C

3.6 Thermal stability studies

To measure the heat flows associated with phase transitions in Ag_2O/TiO_2 heterostructure and as-synthesized TiO2 nanobelt as a function of time or temperature, we used differential scanning calorimetry (DSC) technique. The calorimetry is particularly applied to monitor the thermal behaviour like changes of phase transitions of the newly synthesized Ag_2O/TiO_2 heterostructures and TiO_2 nanobelt (Skoog *et al*. 1998). The samples with a mass of 20 mg were placed in aluminium crucible. The experiments were performed in synthetic air (flow rate of 1.67 cm3 s-1) at 10 °C/min heating rate up to 500 °C. Fig. 7 reveals the endothermic decomposition nature of Ag_2O/TiO_2 heterostructures which includes the thermal decomposition of water molecules present in the material at 100 °C and phase transition at ~ 450 °C (Skoog *et al*. 1998).

3.7 Photocatalytic studies

To assess the photocatalytic degradation capability of Ag_2O/TiO_2, we examined the decomposition of methylene blue (MB) in water under UV-Visible light irradiation as a function of time. MB monomer consists of a sharp intense peak at 670 nm and a shoulder at 610 nm which corresponds to 0-1 vibronic transition in water (Bergmann and O'Konski, 1963). When the experiment was carried out with catalyst but in the absence of light irradiation, no change in methylene blue concentration was observed. Consequently, the decrease of concentration is attributed to the photocatalytic process. The Ag_2O/TiO_2 heterostructure photocatalyst exhibited a 6-fold high activity for MB degradation under UV irradiation (fig. 8). More interestingly, the entire characteristic band of MB at ~ 670 nm showed a red shift (725 nm) due to enhanced intermolecular cross relaxation of the excitation energy (Wang Ya-Lan *et al*. 2013).

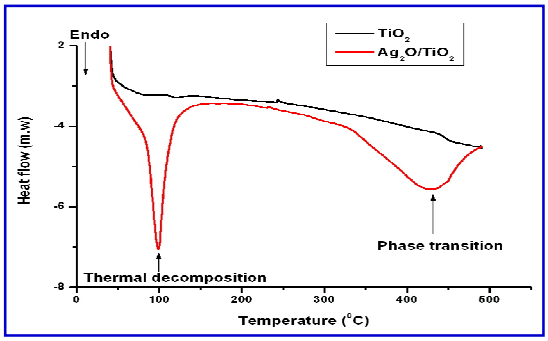

Fig. 7: Differential Scanning Calorimetry spectrum recorded for as-synthesized TiO_2 nanobelt and Ag_2O/TiO_2 heterostructure in an air stream at a heating rate of 10 °C/min.

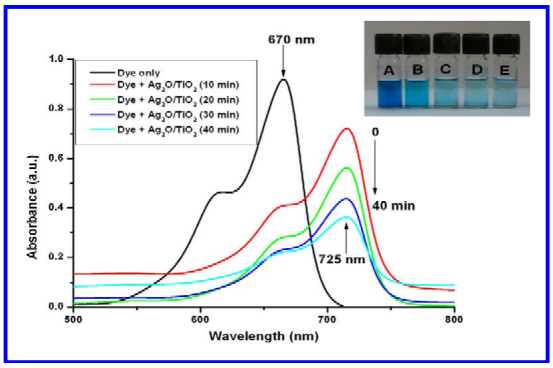

Fig. 8: Photocatalytic degradation of Methylene blue in the presence of Ag_2O/TiO_2 heterostructure under UV-Visible light irradiation; (inset) Color degradation of MB with respect to time interval: (A) dye only; (B) dye+Ag2O/TiO2 (10 min stirring); (C) dye+Ag_2O/TiO_2 (20 min stirring); (D) dye+Ag_2O/TiO_2 (30 min stirring); (E) dye+Ag_2O/TiO_2 (40 min stirring).

With the irradiation time increasing, the decomposition of MB dye progressed steadily and 90% completed in 40 min of UV light irradiation. The degradation activity of Ag_2O/TiO_2 heterostructure photocatalyst was much higher than those of the TiO_2 nanobelts, and the corresponding degradation rates were only ~10% after the same experimental time (SI Fig. 2). The heterostructure between Ag_2O and TiO_2 causes the enhanced photocatalysis activity of the catalysis. To reuse a photocatalyst, the photocatalyst must be easily separated from the reaction medium and maintain its activity. The Ag_2O/TiO_2

heterostructure displayed an extraordinary high stability and recyclability. It can be easily separated by simple centrifuge technique due to its large particle size. Moreover, even though the composite had been reused four times, it still exhibited high photoactivity. The enhanced performance of Ag_2O/TiO_2 heterostructure could be attributed to its unique surface and electronic properties that substantially affected the photocatalytic processes involved in the degradation, including generation of charge−hole pairs, transfer and trapping of charge carriers, and recombination of charge−hole pairs (Li and Gray, 2007).

4. CONCLUSION

We have reported a very simple and novel method to prepare Ag_2O/TiO_2 heterostructure using as-synthesized TiO_2 nanobelt, which was synthesized by sequential autoclaving of TiO2 at 200 ^oC for 48 h in the presence of 10 M NaOH solution. The preliminary characterization studies such as UV-visible absorption, particle size analyzer, zeta potential are in good agreement with the formation of stable Ag_2O/TiO_2 nanobelt. Highly stable and monodispersed nature of Ag_2O/TiO_2 heterostructure was confirmed by the zeta potential and electrophoretic mobility values, respectively. The X-ray diffraction study results prove the high crystalline nature of Ag_2O/TiO_2 heterostructure which could be a good candidate for the various industrial applications. The surface morphology study results give important information that less surface area coating Ag_2O/TiO_2 nanobelt can be a good catalyst for the heterogeneous reactions. Furthermore, the photocatalytic studies revealed that Ag_2O/TiO_2 heterostructure is a stable photocatalyst for MB dye degradation within short period of time. Diverse kind of biological activity tests are ongoing in our laboratory and the results will be published in due course.

REFERENCES

Bergmann, K. and O'Konski, C. T., A Spectroscopic study of methylene blue monomer, dimer and complexes with montmorillonite, *J. Phys. Chem.* 67, 2169(1963). doi: 10.1021/j100804a048

Dai, Y. Q., Cm. M. Cobley, Zeng, J., Sun, Y. M. and Xia, Y. N., Synthesis of Anatase TiO_2 Nanocrystals with Exposed {001} Facets, *Nano Lett.* 9, 2455(2009). doi: 10.1021/nl901181n

Dodda, A., McKinleya, A., Tsuzuki, T. and Saunders, M., Optical and photocatalytic properties of nanocrystalline TiO 2 synthesised by solid-state chemical reaction,*J. Phys. Chem. of Sol*. 68, 2341(2007). doi:10.1016% 2fj.jpcs. 2007. 07 .008

Hegde, M. S., Nagaveni, K. and Roy, S., Synthesis, structure and photocatalytic activity of nano TiO2 and nano Ti1−xMxO2−δ (M = Cu, Fe, Pt, Pd, V, W, Ce, Zr), *J. Physics* 65, 641(2005).

Henderson, M. A., White, J. M., Uetsuka, H. and Onishi, H., Photochemical Charge Transfer and Trapping at the Interface between an Organic Adlayer and an Oxide Semiconductor, *J. Am. Chem. Soc.* 125, 14974(2003). doi: 10.1021/ja037764+.

Hu, A., Liang, R., Zhang, X., Kurdi, S., Luong, D., Huang, H., Peng, P., Marzbanrad, E., Oakes, K. D., Zhou, Y. and Servos, M. R., Enhanced photocatalytic degradation of dyes by TiO2 nanobelts with hierarchical structures, *J. Photochem. Photobio. A: Chem.*, 256, 7(2013). doi: 10.1016/j.jphotochem.2013.01.015.

Lazzeri, M., Vittadini, A. and Selloni, A., Structure and energetics of stoichiometric TiO_2 anatase surfaces, *Phys. Rev. B* 63, 155409(2001). doi:10.1103/PhysRevB.63.155409

Li, G. and Gray, K. A., The solid-solid interface: explaining the high and unique photocatalytic reactivity of TiO_2-based nanocomposite materials, *Chemical Physics*, 339, 173*(*2007). doi:10.1016/j.chemphys.2007.05.023

Li, G., Ciston, S., Saponjic, Z. V., Chena, L., Dimitrijevic, N. M., Rajh, T. and Graya, K. A., Synthesizing mixed-phase TiO_2 nanocomposites using a hydrothermal method for photo-oxidation and photoreduction applications, *J. Catalysis*, 253, 105(2008). doi:10.1016/j.jcat.2007.10.014

Linsebigler, A. L., Lu, G. and Yates, J. T., Jr., Photocatalysis on TiO2 Surfaces: Principles, Mechanisms, and Selected Results,*Chem. Rev.* 95, 735(1995). doi: 10.1021/cr00035a013

Liu, Y., Shu, W., Chen, K., Peng, Z. and Chen, W., Enhanced Photothermocatalytic Synergetic Activity Toward Gaseous Benzene for Mo+C-Codoped Titanate Nanobelts, *ACS Catal.* 2, 2557(2012). doi: 10.1021/cs300501e

Mukhopadhyay, A., Basak, S., Kishore Das, J., Medda, S. K., Chattopadhyay, K. and De, G., Ag−TiO_2 Nanoparticle Codoped SiO_2 Films on ZrO_2 Barrier-Coated Glass Substrates with Antibacterial Activity in Ambient Condition, *ACS Appl. Mater. Interfaces*, 2, 2540*(*2010). doi: 10.1021/am100363d

Skoog, D. A., Holler, F. J. and Nieman, T., *Principles of Instrumental Analysis* (5 edn.), NewYork, pp. 805(1998). ISBN:0030020786

Sze-Mun Lam, Jin-Chung Sin, Ahmad Zuhairi Abdullah, Abdul Rahman Mohamed, Efficient photodegradation of resorcinol with Ag_2O/ZnO nanorods heterostructure under a compact fluorescent lamp irradiation, *Chemical Papers-Slovakacademy of Sciences*, 67(10) 1277–1284(2013). doi:10.2478/s11696-013-0395-8.

Wang Ya-Lan, Zhou Zhang-Kai, Peng Xiao-Niu, Zhou Li, Hao Zhong-Hua and Wang Qu-Quan, The Fluorescence Dynamics of Chlorophyll *a* and Sodium Magnesium Chlorophyllin, *Chin. Phys.Lett.* 30, 098702 (2013). doi:10.1088/0256-307X/30/9/098702

Wang, J., Tafen, D. N., James P. Lewis, Hong, Z., Manivannan, A., Zhi, M., Li, M. and Wu, N., *J. Am. Chem. Soc*. 156, 345 (2009).

Wang, Y., Du, G., Liu, H., Liu, D., Qin, S., Wang, N., Hu, C., Tao, X., Jiao, J., Wang, J. and Wang, Z. L., Nanostructured Sheets of Ti —O Nanobelts for Gas Sensing and Antibacterial Applications†, *Adv. Funct. Mater*. 18, 7(2008). doi: 10.1002/adfm.200701120

Xiong, Z. and Zhao, X., Nitrogen-Doped Titanate-Anatase Core–Shell Nanobelts with Exposed {101} Anatase Facets and Enhanced Visible Light Photocatalytic Activity, *J. Am. Chem. Soc*. 134, 5754 (2012). doi: 10.1021/ja300730c

Xu, F., Benavides, J., Ma, X. and Cloutier, S. G., Interconnected T i O2 Nanowire Networks for PbS Quantum Dot Solar Cell Applications, *J. Nanotech*. Article ID 709031(2012). doi.org/10.1155/2012/709031

Zhou, W., Liu, H., Robert I. Boughton, Du, G., Lin, J., Wang, J. and Liu, D., One-dimensional single-crystalline Ti–O based nanostructures: properties, synthesis, modifications and applications, *J. Mater. Chem*. 20, 5993(2010). doi: 10.1039/B927224K

Zhou, W., Liu, H., Wang, J., Liu, D., Du, G. and Cui, J., *ACS Appl. M ater. & Interfac.* 23, 394(2004).